Aeroacoustics of Aeolian Tones and Effects of Periodic Holes.

R.F. Jones[1]

[1]Student, Department of Mechanical Engineering

University of Adelaide, Adelaide, South Australia, 5005 AUSTRALIA

Abstract

CFD techniques are applied to a cylinder in cross flow and Computational AeroAcoustic (CAA) capabilities developed. Using Curle's method, radiated noise is calculated for solid cylinders and attenuation due to periodic holes is investigated. The numerical analysis exhibits a relationship between hole size and noise attenuation and shows that momentum addition to the wake destructively interferes with the sound sources.

Nomenclature

a	=	Free stream velocity
δ_{ij}	=	Surface area for element ij.
dx	=	step in x direction
F	=	Body forces
f	=	Arbitrary function
n	=	Normal vector to the surface of the region
p	=	Pressure
ρ	=	Density
r	=	Distance to observer
S	=	Body surface
T	=	Reynolds Stress Tensor
t	=	Time
τ	=	Retarded time
τ_{ij}	=	Shear stress
V	=	Body volume

Introduction

As transportation vehicle speeds have increased, so too has associated undesirable aerodynamic noise. This noise is a concern for both passengers and surrounding observers. Of particular relevance to this project is high-speed train pantograph noise, however the results may be applied to other situations involving cylinders in cross flow such as aircraft landing gear or radio antennae.

This noise generated by an object moving in fluid is termed aeroacoustics, and in order to better understand the noise generating mechanism the moving body of fluid may be considered in three regions: the near field where a majority of the turbulence and noise sources occur; a transition region; and the far field region where acoustic waves proporgate to the listener. These regions of fluid motion are analogous to the flows occuring in a small water fall. At the base of the water fall is the near field turbulent region, where dynamic fluid motion is dominant. Beyond the near field is a transition region containing some turbulence and sporadic surface waves. Extending further over the body of water propagating surface waves can be seen, representing the acoustic pressure waves in the far field. While there are differences between this example and that of acoustic wave propagation (transverse surface waves versus longitudinal pressure waves), the principle remains that far field waves are caused by sources in the near field. For this reason it is in our interest to reduce noise at the source, rather than addressing noise at the observer.

Theory

There are two primary methods of solving for aerodynamic sound. The first is Direct Numerical Simulation (DNS) where all flow features (including acoustic) are solved for from the governing equations. The second splits the near field from the far field, solves for source terms in the near field, using them to approximate the far field acoustics, commonly termed acoustic analogies. Lighthill [8] pioneered the field of aeroacoustics with his reformulation of the Navier-Stokes equations. No assumptions are made in the derivation of Lighthill's acoustic analogy, and therefore it still contains all of the flow characteristics such as convection and diffusion. However, in the presence of surfaces the sound field will change. In order to address this situation there are a number of other scalar acoustic analogy methods which have included surface source terms by further manipulation of Lighthill's formulation. Contributors to the acoustic analogies following Lighthill include Curle [2], Ffowcs Williams [5], Phillips [5] and Lilley [5].

Curle [2] was the first to develop an analytical equation which accounts for surface source terms. Ffowcs Williams took a more mathematical approach in rewriting the governing equations using generalized functions. The wave equation is developed and the solution found by convolution by Green's function. Further still, Phillips seeks a solution for cases where the mean flow is non-zero, and with variable density or variable temperature. However, Phillips' analogy fails to account for acoustic propagation through shear layers, a problem which Lilley then addresses by further manipulation. While a full overview and derivation of all methods is outside the scope of this paper, Curle's method remains valid for a stationary observer and low Mach number and his final result is,

$$\rho(x,t) - \rho_0 = \frac{1}{4\pi a_\infty^2} \frac{\partial^2}{\partial x_i \partial x_j} \int_V \frac{T_{ij}}{r} dV$$

$$-\frac{1}{4\pi a_\infty^2} \frac{\partial}{\partial x_i} \int_S \frac{n_j}{r}(p\delta_{ij} - \tau_{ij})dS$$

(1)

For a full derivation of Curle's equation and other acoustic analogies, please refer to Larsson [5]. It should be noted at this point that the first term in Curle's equation represents a volume or quadrupole source term, and the second represents a surface or dipole source term.

This is an important point because dipole source terms (proportional to velocity to the sixth power) are far more efficient noise sources than quadrupole terms [1] (proportional to velocity to the eighth power). Therefore for certain situations where surfaces sources dominate the radiate sound, the quadrupole terms in Curle's equation may be neglected.

Further consideration must be made for actually implementing Curle's equation. By assuming that distance to the observer is much larger than the size of the sources (which is true for the observer in the far field) then the spatial derivatives may be converted into temporal ones since,

$$\frac{\partial f(\tau)}{\partial x_i} = -\frac{1}{a_\infty} \frac{\partial r}{\partial x_i} \frac{\partial f}{\partial \tau}$$

(2)

From this position a number of reformulations have been made by researchers, depending on the purpose of their studies and what form their source term data takes (time or frequency dependent). For example the Doppler effect can be taken into account while reformulating Curle's equation such that it can be applied to time dependent force data for a cylinder in cross flow [3], while others have reformulated Curle's equation such that frequency dependent source data might be used [7]. Since the flow simulations in this project will generate force data on the surface of the cylinder at each time step, a time dependent form of Curle's equation [4] can be used in the following form,

$$p(x,t) = \frac{x_i}{4\pi a_\infty |x|^2} \frac{\partial F_i(\tau)}{\partial \tau}$$

(3)

It should be noted that a major assumption with Eq. 3 is that the body is acoustically compact (*i.e the body is smaller than a quarter of the wavelength*).

A number of studies have been conducted on the cylinder in cross flow problem; these compare Curle's method with DNS results [3,9]. In these papers, Curle's method was found to compare very well with DNS results and the importance of the Doppler effect at low Mach numbers is discussed. While Larsson [5] does not take into account Doppler effects, Curle's method was still found to agree well with DNS [3]. Therefore since the

direct numerical simulation predicts the flow field very accurately, then it can be concluded that Curle's method and the assumptions made are appropriate for a cylinder in cross flow.

Results and Discussion
Laminar Simulations

The purpose of the laminar simulations was to determine the suitability of various domain geometries for aeroacoustic analysis. The desired domain must be easy to code, have little influence on results due to boundary effects and adequately capture the wake dynamics. The expected flow structure at a Reynolds number of 200 is a laminar Von Karman vortex street [10], resulting in periodically varying cylinder forces and hence a dipole sound source. A number of geometrical configurations were explored, including circular, square and rectangular domains. All variations passed meshing requirements such as aspect ratio, orthogonality, area and angle skew; however it was immediately clear that the easiest domain to code and manipulate consisted of two squares, the first square containing the cylinder and the other extending the wake region as shown in Fig. 1.
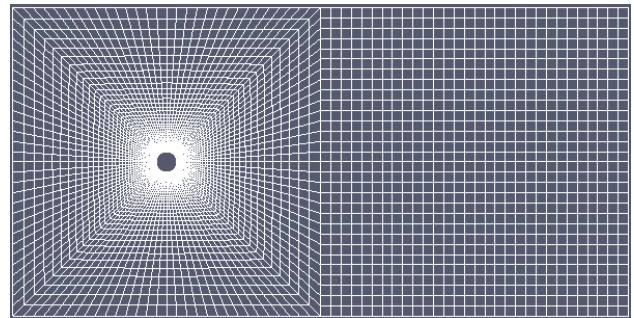

Figure 1. Diagram of the two-squares computational domain.

For these reasons, the two-squares domain shape was used from this point forward. The OpenFOAM laminar flow solver [11] was then run and cylinder forces output to the log file at each time step, while the initial residuals were monitored for convergence. Discretization errors were addressed by refining the grid and noting the mean drag force. Grid Convergence Index (GCI) [12] was then applied to the mean drag force; the results can be seen in Table 1 and the associated meshes in Fig. 2.

Mesh	Φ_h	p	ε_h	GCI %
Very Coarse	1.5056	-	-	-
Coarse	1.4376	-	-0.047	3.61
Medium	1.4104	0.66	-0.019	1.47
Fine	1.4006	0.74	-0.007	0.53

Table 1. GCI values for grid refinement, Φ_h = mean drag coefficient, ε_h = fractional error for a grid with spacing h, **p** = order of the method (after Wilcox [12]).
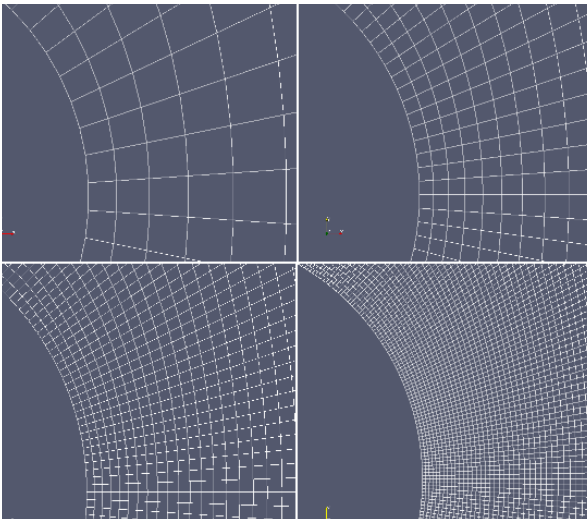
Figure 2. Very Coarse, coarse, medium and fine meshes.

The Von Karman vortex street can be clearly seen in Fig. 3. Discretization errors estimated by using the GCI shows that the grid is 1st order accurate, with very low errors. The modeling error is small since the mean drag coefficient is very close to the published value of 1.5 for a Reynolds number of 200 [10].
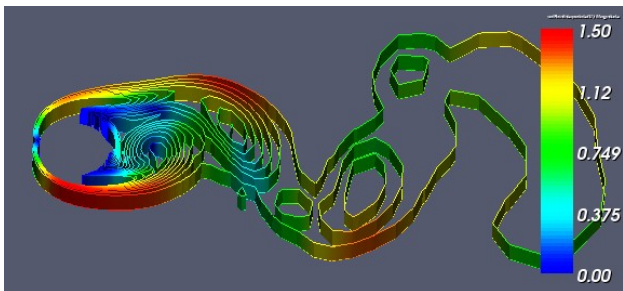

Figure 3. Colour contour plot of vorticity for cylinder in cross flow at Re = 200.

The CFD solution is of excellent quality: overall the two-squares rectangular domain proved to be extremely efficient due to the ease of implementation and meshing, no requirement for orthogonal correctors and ability to capture an extended region of the wake.
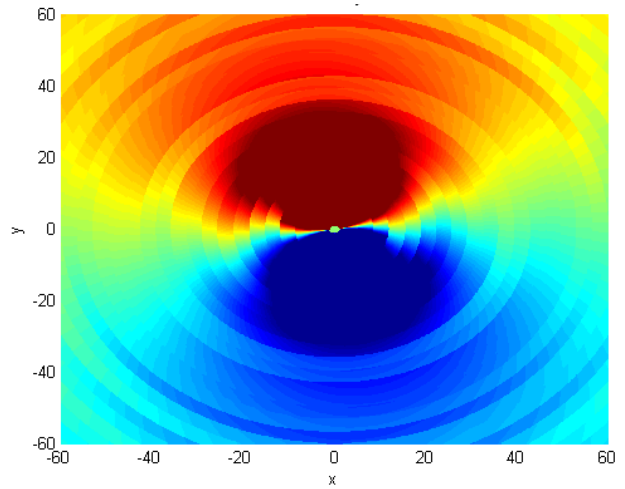
Figure 4. Acoustic field surrounding cylinder at Re = 200. Note that x and y dimensions are normalized by the radius.

The force data was then input into Curle's equation producing the acoustic field, which can be seen in Fig. 4, and the associated spectra in Fig. 5. This spectra shows a peak at a Strouhal number of 0.2, which corresponds with the expected Strouhal number for cylinder flow. This first peak is attributed to the fluctuating lift frequency, while the harmonics are due to fluctuations in drag coefficient being twice the frequency of lift. Noise with spectra such as this is tonal in nature, and can be very annoying to the receiver. The acoustic solution confirms that the cylinder acts as a dipole source, and exhibits the appropriate sound field.
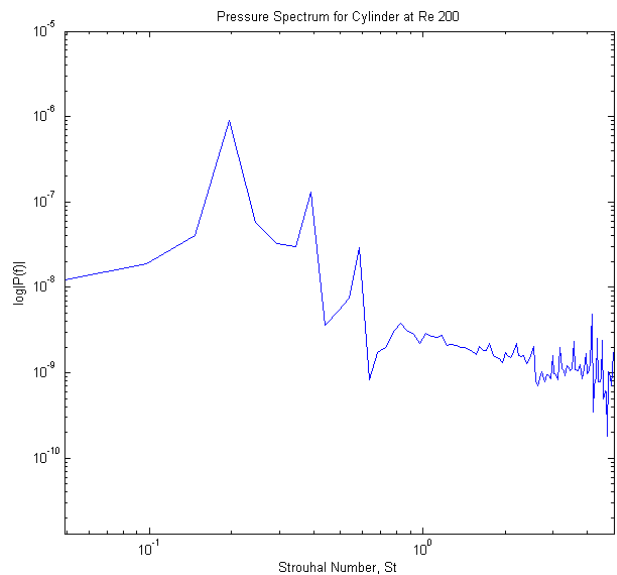

Figure 5. Acoustic pressure spectrum for cylinder at Re = 200.

Turbulent 2D Simulations

The purpose of conducting turbulent simulations of a 2D cylinder in cross flow at a Reynolds number of 10 000 is to test the method, using a Reynolds number for more realistic flow situations and check that Curle's method is a valid tool for differentiating between the acoustic properties of different geometries. These simulations required a turbulent model capable of handling the transient nature of the problem, namely Unsteady RANS.

The expected wake structure will be the turbulent Von Karman vortex street [10], again resulting in periodically varying cylinder forces and hence a dipole sound source. Flow at Re = 10 000 was chosen because the turbulent Von Karman vortex street is observable at this value, and there is published experimental data available for validation of the model [6].

The model was set up using a standard k-epsilon turbulence solver, with due attention given to iteration and convergence criteria. An additional consideration is the y+ value of the mesh. Because the cylinder uses a wall function, y+ is required [12] to be between 10 and 100. However due to the vortex shedding and the intimate relationship between boundary layer resolution and surface forces [12], the y+ value was maintained at approximately 1. A full second order scheme was used in these simulations; this was required because first order schemes did not produce the expected cylinder forces. A plot of vorticity can be seen in Fig. 6. Again the dipole sound source can be seen in Figure 7 for the turbulent flow regime.
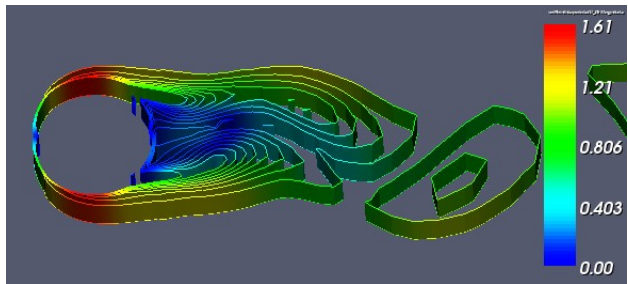

Figure 6. Colour contour plot of vorticity for cylinder in cross flow at Re = 10 000.

The acoustic field was determined, and a plot of the radiating acoustic field can be seen in Fig. 6. Additionally, the spectra for the turbulent case, Figure 8, shows a reduction in harmonics of the lift frequency, due to the fact that vorticies tend to be convected downstream due to the high momentum of the fluid before they can grow too large. This leads to near constant drag forces, and hence less harmonics.
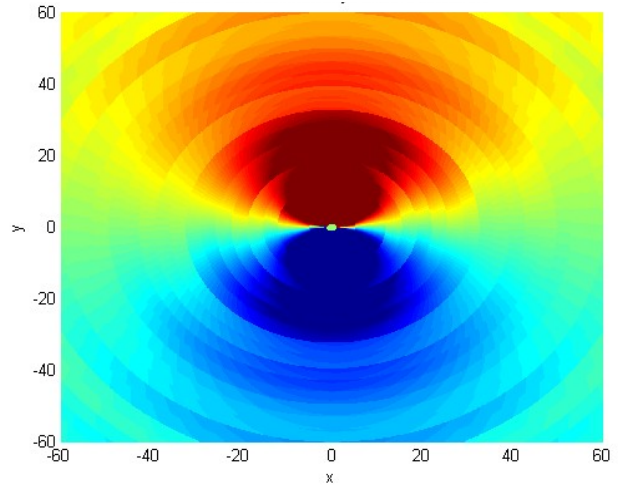

Figure 7. Acoustic field for cylinder at Re = 10 000.
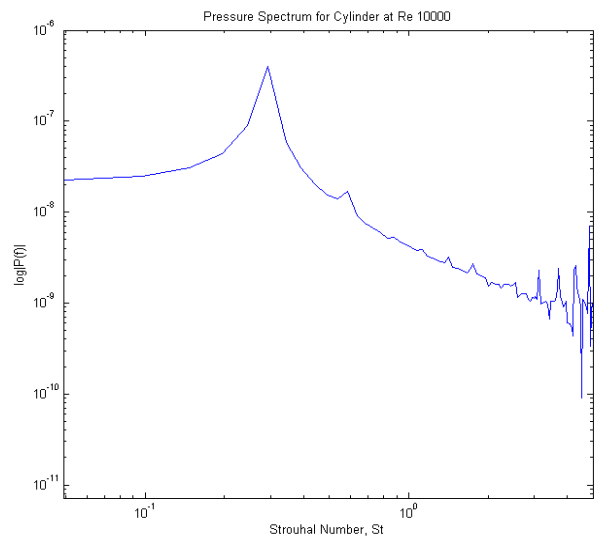

Figure 8. Acoustic pressure spectrum for cylinder at Re = 10 000.

Holes were then added to the 2D cylinder in order to investigate the relationship between hole width and noise suppression, see Figs. 9 and 10. The spectra has completely changed, and a receiver would no longer experience the tonal noise as for a solid cylinder.
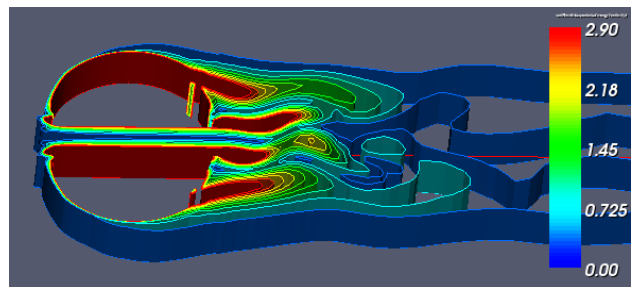

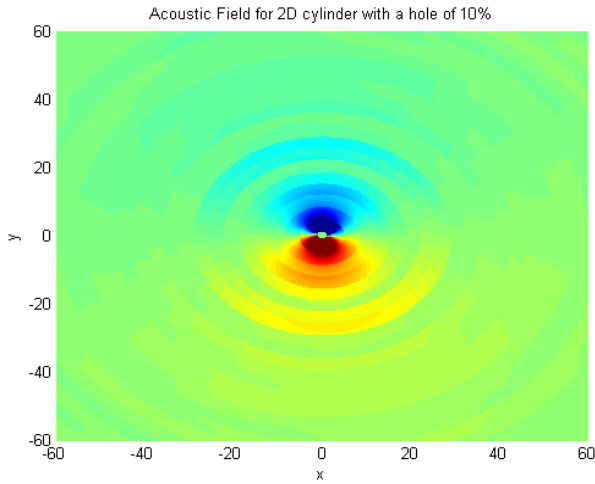Figure 9. Colour contours of vorticity for cylinder with hole 7.5% of diameter, Re = 10 000.

687

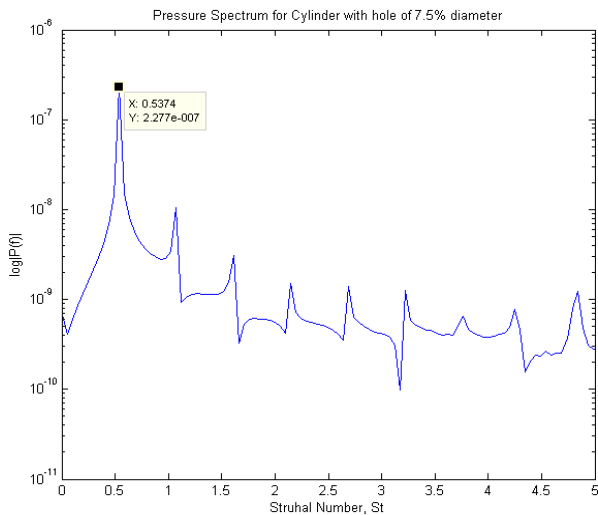Figure 10. Acoustic field for cylinder with hole 7.5% of diameter, Re = 10 000.

Figure 11. Acoustic pressure spectrum for cylinder with hole 7.5% of diameter, Re = 10 000.

Widths between 3.5% and 15.5% of the cylinder diameter were analyzed. It was observed for hole widths above 10% of the cylinder diameter, at a Reynolds number of 10 000, recirculation bubbles form behind each half circle and there is no observable wake instability. Since Curle's method requires fluctuating surface forces for noise generation, it is concluded that for hole widths above 10% virtually all noise is eliminated (except for acoustically weak quadrupole terms formed in the wake). Various geometries were tested at 0.5% intervals between 3.5 and 15.5% of the diameter. As expected the results show an addition of fluid momentum to the wake, and a subsequent reduction in fluctuating body forces. To demonstrate this, RMS lift coefficient was plotted against the width of the hole as a percentage of cylinder diameter, Fig. 12. Interestingly, for small holes there is an increase in fluctuating forces. This is attributed to a whistling type phenomena, however further simulations are required to determine the nature of the sound to the ear. Widening of the slots shows a decline in fluctuating forces and hence noise. This coincided with formation of stable recirculation bubbles behind each half of the cylinder, after which further momentum addition to the wake did not have any effect.
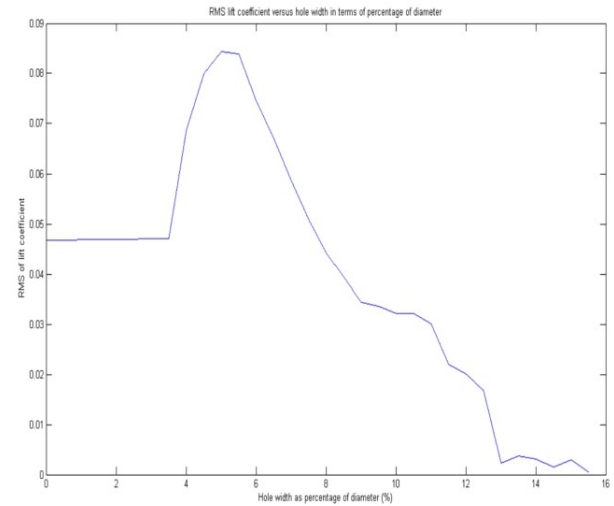

Figure 12. RMS of lift coefficient versus hole width, 2D simulations. Re = 10 000.

Turbulent 3D Simulations

The geometry was extended in the z-direction so that the results may be directly applied to train pantograph design. Production of a quality 3D mesh of a cylinder with periodic holes proved to be a difficult exercise. Hence when a consistent mesh for one configuration was found, a program was written to take an input file describing a periodic hole configuration, calculate the required mesh attributes and output a mesh file ready for simulation.

This proved an invaluable tool when conducting numerous simulations. However due the highly demanding computing time required for these simulations, only preliminary results are available at this stage. A contour plot of vorticity for one configuration is shown in Fig. 13, where the additional fluid momentum can be seen breaking up the wake structure. The cylinder force coefficient results of two hole configurations are depicted in Figs 14 and 15. Note only the first 100 seconds have been simulated. The initial drag response can be seen to increase rapidly as separation bubbles form behind the cylinder. After approximately 50 seconds the wake becomes unstable, as indicated by the fluctuating lift. Again there appears to be a strong relationship between hole area and noise suppression as the larger holes resulted in an obvious reduction in fluctuating forces.
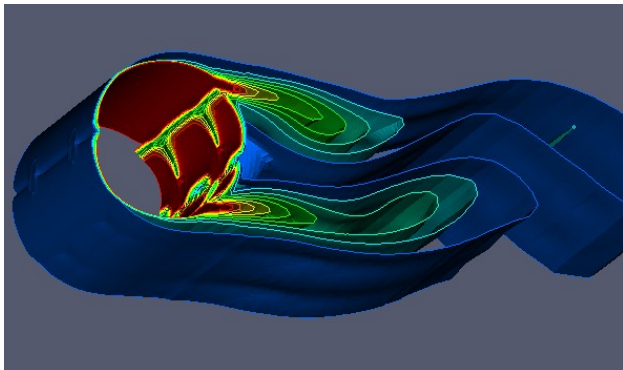
Figure 13. Vorticity contours for cylinder with periodic holes of width, height and distance between centers of 5%, 10% and 100% of the diameter respectively. Re = 10 000.
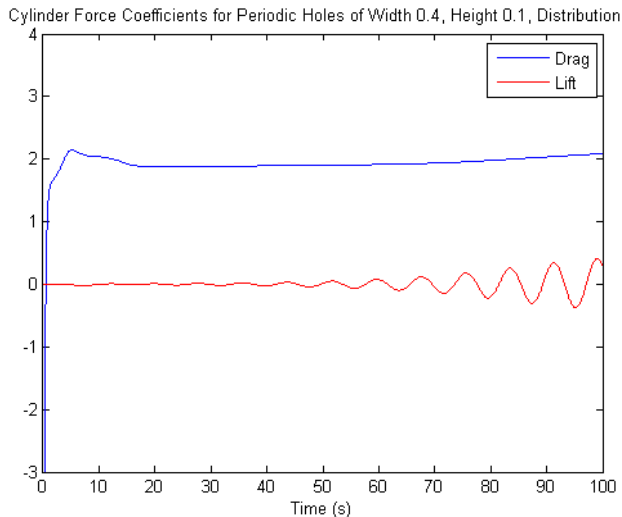

Figure 14. 3D Cylinder force coefficients for periodic holes of height, width and distance between centers of 5%, 10% and 100% diameter respectively. Re = 10 000.
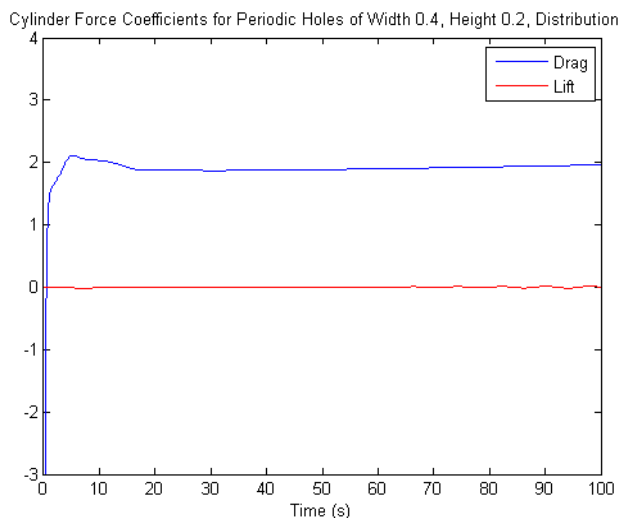

Figure 15. 3D Cylinder force coefficients for periodic holes of height, width and distance between centers of 10%, 10% and 100% diameter respectively. Re = 10 000.

Conclusion

Curle's analogy allows for aeroacoustic prediction of noise from cylinder flow, and exhibits the expected dipole sound field. Breaking up the wake structure by indroducing holes in the cylinder has an effect on the fluctuating surface forces. Fluctuations are increased for relatively small holes, and decreased for larger holes.

Since radiated noise is directly related to the fluctuating surface forces by Curle's equation, noise is attenuated for these larger holes. Also there appears to be a cut-off point where further addition of momentum to the wake region does not improve noise attenuation. It is expected that further investigations will show a definite relationship between percent open area and noise reduction, and further exploration of periodic holes in 3D will allow for the results to be directly applicable to some aeroacoustic noise problems.

Acknowledgments

References

[1] Bies, D.A. and Hansen, C.H., *Engineering Noise Control: Theory and Practice*, Spon Press, 2003.

[2] Curle, N., *"The Influence of Solid Boundaries Upon Aerodynamic Sound,"* Proceedings of the Royal Society, Series A 231, 505-514, 1955.

[3] Hatakayama, N. and Inoue, O. *"Sound Generation by a two-dimensional circular cylinder in a Uniform Flow,"* Journal Fluid Mechanics, Vol. 471, pp 285-314, 2002.

[4] Howe, M.S., *Acoustics of Fluid Structure Interaction*, Cambridge University Press, 1998.

[5] Larsson, J., *"Computational Aeroacoustics for Vehicular Applications,"* PhD Thesis, Chalmers University of Technology, 2002.

[6] Leclercq, D.J.J., Doolan, C. and Reichl, J., *"Development and Validation of a Small-Scale Anechoic Wind Tunnel,"* 14th International Conference on Sound and Vibration, 2007.

[7] Leclercq, D.J.J. and Symes, M.K. *"Predicting the Noise Generated by a Bluff Body in a Fluctuating Flow,"* 10th AIAA/CEAS Aeroacoustics Conference, AIAA 2004-2917, 2004.

[8] Lighthill, M.J., *"On Sound Generated Aerodynamically – I: General Theory,"* Proceedings of the Royal Society, Series A 221, 564-587, 1952.

[9] Moon, Y.J. and Seo, J.H., *"Perturbed Compressible Equations for Aeroacoustic Noise Prediction at Low Mach Numbers,"* AIAA Journal, Vol. 43, No8, 2005.

[10] Munson, B.R., Young, D.F. and Okiishii, T.H., *Fundamentals of Fluid Mechanics*, John Wiley & Sons Inc, 5th ed., 2006.

16th Australasian Fluid Mechanics Conference

Crown Plaza, Gold Coast, Australia

2-7 December 2007

[11] OpenFOAM Limited, *OpenFOAM: The Open Source CFD Toolbox – Users Guide*, OpenCFD Ltd, Version 1.3, November 2006.

[12] Wilcox, D.C., *Turbulence Modelling for CFD*, 2nd ed., DCW Industries, 1998.